MANOEUVRABILITY ASSESSMENT OF A HYBRID COMPOUND HELICOPTER CONFIGURATION

Kevin Ferguson
k.ferguson.1@research.gla.ac.uk
Ph.D Student
University of Glasgow
Glasgow, United Kingdom

Douglas Thomson
Douglas.Thomson@glasgow.ac.uk
Senior Lecturer
University of Glasgow
Glasgow, United Kingdom

ABSTRACT

The compound helicopter design could potentially satisfy the new emerging requirements placed on the next generation of rotorcraft. The main benefit of the compound helicopter is its ability to reach speeds that significantly surpass the conventional helicopter. However, it is possible that the compound helicopter design can provide additional benefits in terms of manoeuvrability. The paper features a conventional helicopter and a hybrid compound helicopter. The conventional helicopter features a standard helicopter design with a main rotor providing the propulsive and lifting forces, whereas a tail rotor, mounted at the rear of the aircraft provides the yaw control. The compound helicopter configuration, known as the hybrid compound helicopter, features both wing and thrust compounding. The wing offloads the main rotor at high speeds whereas two propellers provide additional axial thrust as well as yaw control. This study investigates the manoeuvrability of these two helicopter configurations using inverse simulation. The results predict that a hybrid compound helicopter configuration is capable of attaining greater load factors that its conventional counterpart, when flying a pullup-pushover manoeuvre. In terms of the Accel-Decel manoeuvre, the two helicopter configurations are capable of completing the manoeuvre in comparable time-scales. However, the addition of thrust compounding to the compound helicopter design reduces the pitch attitude required throughout the acceleration stage of the manoeuvre.

NOMENCLATURE

g	acceleration due to gravity (m/s^2)
$\mathbf{h}$	angle of attack function
k	time point counter
n_{fp}	flight path load factor
n_{max}	maximum normal load factor
n_p	normal flight path load factor
n_t	tangential flight path load factor
$\bar{r}$	radial station along the rotor blade
S	Accel-Decel distance (m)
t	time (s)
$\mathbf{u}$	control vector (rad)
V	aircraft flight speed (m/s)
$\dot{V}$	aircraft acceleration (m/s^2)
x, y, z	manoeuvre flight path co-ordinates (m)
$\mathbf{x}$	state vector (various units)
$\dot{x}, \dot{y}, \dot{z}$	earth axes velocities (m/s)
$\ddot{x}, \ddot{y}, \ddot{z}$	earth axes accelerations (m/s^2)
$\mathbf{y}_{des}$	trajectory definition matrix (various units)

α_e	trimmed angle of attack, W_e/U_e (rad)
α'	angle of attack excursion (rad)
χ	track angle (rad)
γ	glideslope angle (rad)
$\dot{\gamma}$	rate of change of the glideslope angle (rad/s)
ψ	heading angle (rad)
θ	Euler pitch angle (rad)
θ_0	main rotor collective pitch angle (rad)
θ_{1s}	main rotor longitudinal pitch angle (rad)
θ_{1c}	main rotor lateral pitch angle (rad)
θ_{diff}	propellers differential control pitch angle (rad)
$\bar{\theta}_{\text{prop}}$	mean propeller pitch angle (rad)

1. INTRODUCTION

The compound helicopter has experienced a resurgence of interest due to its ability to obtain speeds that significantly surpass the conventional helicopter. This increase in speed makes the compound helicopter suit-

able for various roles and missions such as troop insertion, search and rescue, ship replenishment as well as short haul flights in the civil market. The compounding of a helicopter is not a new idea but the development of a compound helicopter has proven elusive for the rotorcraft community due to a combination of technical problems and economical issues[1]. The rotorcraft community is again exploring the compound helicopter design, with various manufacturers testing their prototypes.

The success of the conventional helicopter is partly to its unique ability to perform precise manoeuvres in Nap of the Earth (NAP) flight. One method of assessing the helicopter's ability to perform manoeuvres is inverse simulation. Inverse simulation reverses the conventional simulation approach by calculating the control activity required to force a vehicle along a particular trajectory[2]. The first inverse simulation algorithm, known as the differentiation method, was developed by Thomson and Bradley[3], to assess helicopter agility of a six degree of freedom (DOF) rotorcraft model. The success of the inverse simulation results, as well as the increasing interest in handling qualities and pilot workload research, prompted future development of the algorithm. Subsequently, inverse simulation has been used for various applications, including investigating pilot control strategies, conceptual design analyses and handling qualities[4–7]. Despite the success of the differentiation method, there were some problems which consequently led to a new approach to inverse simulation. The major limitation of the differentiation method was that the mathematical model and the algorithm were strongly coupled, therefore even slight changes to the mathematical model required alterations to the algorithm itself. Realising this shortcoming, Hess, Goa and Wang developed a generalised technique of inverse simulation[8], often referred to as the integration method, which fully separates the mathematical model from the algorithm. Due to the robust and flexible nature of this technique, the integration method has become the most common approach[9]. Before proceeding, another two methods of solving the inverse problem should be noted. Firstly, the two time-scale method, as described by Avanzini and de Matteis[10], assumes that the rotational dynamics of an aircraft are much quicker than the translational dynamics, therefore permitting the assumption that the main rotor collective controls the translational dynamics whereas the cyclic and pedals influence the rotational dynamics. This method, similar to the other methods, use iterative schemes, such as the Newton-Raphson method, in order to solve the inverse problem. However, the Newton-Raphson method can be replaced with an optimisation algorithm in order to calculate the control angles, with Celi and de Matteis

et al.[11,12] successfully implementing optimisation algorithms in their respective approaches. The optimisation approach to inverse simulation is particularly useful to problems featuring control redundancy, however an appropriate cost function must be formed.

In terms of manoeuvrability, it is an important design feature if the helicopter is to operate in tight Nap of the Earth (NoE) scenarios[13]. The ability for the helicopter to manoeuvre quickly and effectively enables the vehicle to quickly reposition. Furthermore, enhancing the manoeuvrability and agility of a helicopter can also aid its survivability with its ability to quickly turn or climb to avoid an attack. Traditionally, the design process has focussed on performance and cost to drive the design of the helicopter. However, for the reasons previously stated, a high level of manoeuvrability has become a key design goal for most designers as it increases mission effectiveness[14]. As there is a demand for conventional helicopters to be manoeuvrable, it is reasonable to expect that operators would expect the same for a compound helicopter. Therefore, this paper presents a manoeuvrability assessment of a compound helicopter and compares the results to a conventional helicopter of similar shape and mass. Before proceeding it is important to highlight that there are various definitions of the term manoeuvrability. Therefore it is necessary to define what is meant by manoeuvrability in this current work. Generally, most authors agree that manoeuvrability is the ability of the aircraft to change its flight path[13,15] with Whalley[16] providing an overview of the various definitions proposed by authors. Whalley also concludes by stating his definition of manoeuvrability, which is the following

"Manoeuvrability is the measure of the maximum achievable time-rate-of-change of velocity vector at any point in the flight envelope."

The aim of the current work is to determine the maximum manoeuvring capability of two aircraft configurations, namely a conventional helicopter configuration and a hybrid compound helicopter configuration. Then to subsequently investigate if the compounding of the conventional helicopter offers an advantage in this regard. Hence, in this context, the term "manoeuvrability" and phrase "maximum manoeuvring capability" are used synonymously throughout the remainder of this paper. The strategy for the current work is to use an established mathematical model of a conventional helicopter (in this case, the AgustaWestland Lynx), and then convert this model to represent a hybrid compound helicopter configuration. The Lynx was chosen as a well established dataset and the model was available[17],. The compound configuration that is examined in the pa-

Fig. 1. Sketch of the Hybrid Compound Helicopter (HCH) Configuration.

per is broadly similar to the Eurocopter X[3] with the preliminary design of the configuration discussed in previous compound helicopter study[18]. This configuration is named the hybrid compound helicopter (HCH) configuration, which features a wing and two propellers, as seen in Figure 1. This compound helicopter configuration is changed as little as possible, relative to the baseline model, to allow for a fair and direct comparison between the results of the two configurations. In order to quantify the manoeuvrability of the aircraft configurations, an inverse simulation algorithm is used to calculate the maximum manoeuvring capability of a conventional helicopter and a hybrid compound helicopter. To do this successfully various elements are required. These are namely: mathematical models, inverse simulation algorithm, manoeuvres definition and a manoeuvrability assessment method. The following section provides an overview of these required elements.

2. METHODOLOGY

2.1 Mathematical Modelling

The compound helicopter model is developed using the helicopter generic simulation (HGS) model[19]. The HGS model is a conventional disc-type rotorcraft model, as described by Padfield[17], and has found extensive use in studies of helicopter flight dynamics. The HGS model is generic in structure, with only the helicopters parameters required to model the vehicle. The main rotor model, within the HGS package, ignores the pitching and lagging degrees of freedom, therefore assuming that the flap dynamics have the most influence in terms of the helicopters flight dynamic characteristics. The flapping dynamics are assumed to be quasi steady, a

common assumption in main rotor modelling, therefore permitting a multi-blade representation of the main rotor. The rotor model neglects the rotor periodicity by assuming that only the steady components of the periodic forces and moments generated by the main rotor influence the helicopters body dynamics. The main rotor is assumed to be centrally hinged with stiffness in flap, with the main rotor chord assumed to be constant. Furthermore, the model also features dynamic inflow and a rotor-speed governor model. One important assumption, within the rotor model, is that the aerodynamics are linear, so that the lift is a linear function of the local blade angle of attack, whereas the drag is modelled by a simple polynomial. Due to this assumption, nonlinear aerodynamics such as retreating blade stall and compressibility are not modelled. To model the nonlinear aerodynamics and rotor periodicity requires an "individual blade model,", examples of which are given by Rutherford, Mansur and Houston[20–22]. Regarding the modelling of the other subsystems of the rotorcraft, the forces and moments of the tail plane, fuselage, and fin are calculated using a series of lookup tables derived from experimental data[17].

One question that naturally arises is the validity of these models and if the results from these rotorcraft models would replicate the real aircraft. In terms of the conventional helicopter, inverse simulation results have shown good correlation for a range of maneuvers[23], giving confidence to the worth of the results produced by the HGS model. The limitations of this type of model are well understood[17] and include the inability to accurately capture off-axis effects and low fidelity at the edges of the flight envelope where, for example, aerodynamic are highly nonlinear. In relation to the compound helicopter models, a strict validation based on the comparison of flight test with simulation results is not possible, as the appropriate data is not yet openly available. However, it is believed that the mathematical models would correctly represent the basic physics of the hybrid compound helicopter.

2.2 Inverse Simulation Algorithm

The inverse simulation algorithm used in this current study is the so called integration method. As this method is well documented in the literature[2,9,24] only a brief description is provided within. The integration method uses numerical integration and conventional simulation to calculate the controls required to move a vehicle through a desired trajectory. The first step is to calculate the control angles that trim the aircraft for the given starting flight speed. Generally, a helicopter can be in trimmed flight when climbing, descending or flying

with a lateral velocity (sideslip). However in this current work the trimmed state corresponds to steady level flight with the body accelerations and the attitude rates equal to zero. The next step, after the calculation of the trim control angles is to define the manoeuvre. The manoeuvre is discretised into a series of discrete time points, t_k, by specifying the time step and calculating the number of points. Subsequently, the manoeuvre can be determined with matrix, $\mathbf{y}_{des}(t_k)$ representing the flight path of the manoeuvre. The manoeuvre can be defined by polynomials that satisfy the requirements of the particular manoeuvre[25], with the mathematical modelling of these manoeuvres detailed later. Starting from the trimmed condition, $\mathbf{u}_e$ is the initial guess to calculate the control vector, $\mathbf{u}$, to force the helicopter to the position of the next time point. A Newton-Raphson technique is used to calculate the control vector to force the vehicle to the next time point to match the desired flight path defined by $\mathbf{y}_{des}(t_k)$. After convergence, this numerical technique moves onto the next time point and repeats the process. The end result is the control activity required throughout the manoeuvre.

2.3 Manoeuvre Modelling

2.3.1 Pullup-Pushover Manoeuvre

The output vector, $\mathbf{y}_{des}$, generally contains the three accelerations in the Earth axes set. The relationship between velocities in the Earth axes set and the trajectory angles are given by

$$\dot{x} = V \cos\gamma \cos\chi \tag{1}$$
$$\dot{y} = V \cos\gamma \sin\chi \tag{2}$$
$$\dot{z} = -V \sin\gamma \tag{3}$$

whereas the accelerations in the Earth axes set are found by differentiation and given by

$$\ddot{x} = \dot{V}\cos\gamma\cos\chi - V\dot{\gamma}\sin\gamma\cos\chi - V\dot{\chi}\cos\gamma\sin\chi \tag{4}$$
$$\ddot{y} = \dot{V}\cos\gamma\sin\chi - V\dot{\gamma}\sin\gamma\sin\chi + V\dot{\chi}\cos\gamma\cos\chi \tag{5}$$
$$\ddot{z} = -\dot{V}\sin\gamma - V\dot{\gamma}\cos\gamma \tag{6}$$

Rearrangement of Equation (3) gives the definition of the glideslope

$$\gamma = -\sin^{-1}\frac{\dot{z}}{V} \tag{7}$$

and the time derivative of the glideslope is

$$\dot{\gamma} = \frac{-\ddot{z}V + \dot{V}\dot{z}}{V^2 \cos\gamma} \tag{8}$$

The track angle, χ, can be determined through Equations (1)-(2). It is therefore clear that if the flight speed and trajectory angle profiles are known then the accelerations in the Earth axes set can be determined.

The manoeuvres studied with this paper are typical conventional helicopter manoeuvres, similar to the Pullup-Pushover and Accel-Decel manoeuvres described in the ADS-33[26] requirements. The Pullup-Pushover manoeuvre involves the aircraft achieving positive and negative load factors. The objective of the Pullup-Pushover manoeuvre, as described in ADS-33[26], is to examine the ability of the aircraft to avoid obstacles during high speed NoE operations. The aircraft begins the manoeuvre at a trimmed condition at a flight speed equal or less to 120 kt. The aircraft is required to achieve a sustained positive load factor in the pull up stage of the manoeuvre. Following this the aircraft is then to transition to a Pushover and achieve a negative load factor then to recover to level flight as quickly as possible. The flight path load factor is defined as

$$n_{fp} = \frac{1}{g}\sqrt{\ddot{x}^2 + \ddot{y}^2 + (\ddot{z} - g)^2} \tag{9}$$

whereas the tangential and normal load factors are given by

$$n_t = \frac{\dot{x}\ddot{x} + \dot{y}\ddot{y} + \dot{z}(\ddot{z} - g)}{g\sqrt{\dot{x}^2 + \dot{y}^2 + \dot{z}^2}} \tag{10}$$

$$n_p = \sqrt{n_{fp}^2 - n_t^2} \tag{11}$$

Through the use of Equations (7)-(11), the normal load factor can be expressed in terms of the trajectory angles and flight speed. Due to the complex nature of these equations a symbolic mathematics package was used to determine this relationship. The end result is a lengthy algebraic expression which can approximated with

$$n_p \approx \frac{V\dot{\gamma}}{g} + \cos\gamma \tag{12}$$

Table 1. Load Factor Boundary Conditions

Variable	$t = 0s$	$t = t_1$	$t = t_2$	$t = t_3$	$t = t_4$	$t = t_5$
n_p	1	n_{max}	n_{max}	0	0	1
$\dot{n}_p$	0	0	0	0	0	0
$\ddot{n}_p$	0	0	0	0	0	0
α	α_e	$\alpha_e + \alpha'$	$\alpha_e + \alpha'$	$\alpha_e - \alpha'$	$\alpha_e - \alpha'$	α_e

To define the manoeuvre, the initial task is to define the flight path boundary conditions in terms of the output variables required. In order to do this the load factor distribution throughout the manoeuvre is determined by applying boundary conditions and therefore allowing the construction of piecewise polynomials to satisfy these conditions. The ADS-33 document specifies the majority of the load factors to be attained throughout the manoeuvre[26]. To meet the desired standards of this manoeuvre, the maximum positive load factor must be attained after 1s of commencing the manoeuvre and sustained for a further 2s. Thereafter, the helicopter transitions from the positive load factor to the lowest load factor within 2s, and maintains this load factor for a further 2s. The specification does not explicitly define an end time of the manoeuvre, a point raised by Celi[27], but does state that after the pushover stage of the manoeuvre the aircraft should "*recover to level flight as rapidly as possible*". The assumption in this current work is that the manoeuvre ends when the aircraft's original flight speed is recovered and returns to a normal load factor of unity. Figure 2 shows a load factor distribution which relates to the desirable standards set in the specification. Between each of the time points there are 6 boundary conditions, as seen in Table 1, to satisfy resulting in a fifth-order polynomial to describe the load factor distribution

$$(13) \qquad n_p = a_0 t^5 + a_1 t^4 + a_2 t^3 + a_3 t^2 + a_4 t + a_5$$

Once the coefficients, a_0, a_1, a_2, a_3, a_4 and a_5, are determined by applying the boundary conditions then the normal load factor distribution throughout the manoeuvre can be calculated. Hence, there are three unknowns in Equation (12), namely V, γ and $\dot{\gamma}$. The next step is to determine the variation of flight speed throughout the manoeuvre. One solution to this is to impose a predetermined profile of flight speed throughout the manoeuvre, however there is very little information regarding the variation of airspeed throughout this manoeuvre. The approach taken in this present work, in order to determine a flight speed profile, is to assume that there is a balance of potential and kinetic energy
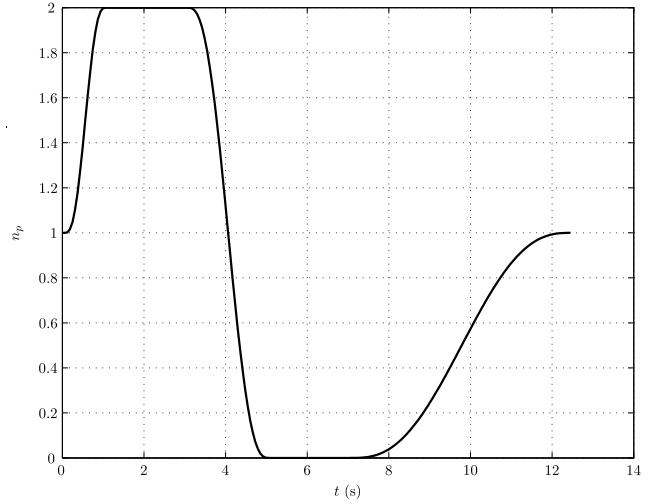
Fig. 2. Desirable Load Factor throughout the Pullup-Pushover manoeuvre.

during the manoeuvre. For example, when the aircraft climbs there is a gain in potential energy which is balanced by a loss of kinetic energy. This assumption of the balance of energy leads to the following equation

$$(14) \qquad \dot{V} = -g \sin \gamma$$

There are now two differential equations, Equations (12) and (14), which can be integrated to determine the flight velocity and climb angle throughout the manoeuvre, using the initial trimmed conditions. As the track angle, χ is set to zero since it is a longitudinal manoeuvre, using the calculated values of V, $\dot{V}$, γ and $\dot{\gamma}$ the accelerations in the Earth axes set can be determined. With the rate of change of heading, $\dot{\psi}$, set to zero, the output vector $\mathbf{y}_{des}$ is now nearly defined allowing it to be used in the inverse simulation algorithm.

As previously discussed, $\mathbf{y}_{des}(t_k)$ is composed of the accelerations of $\ddot{x}_e$, $\ddot{y}_e$ and $\ddot{z}_e$ relative to the Earth axes set. Furthermore, since the conventional helicopter features four controls then the condition of zero heading or sideslip is included so that the output vector contains four elements. However, the extra control of the HCH configuration relative to that of the

BL configuration presents the problem of including an extra constraint in the output vector to find a unique solution of the control vector at each time point. In terms of the Pullup-Pushover manoeuvre, the extra constraint is selected to be $\dot{\alpha}$. Alternatively, a control such as θ_{1s} could be scheduled or fixed throughout the manoeuvre. However, the justification for scheduling $\dot{\alpha}$ is that it is likely a pilot would adopt a control strategy which exploits the lifting capability of the wing in the pull up stage of the manoeuvre. It is found by experimentation by including $\dot{\alpha}$ as an additional constraint and appropriately scheduling this value over the duration manoeuvre results in the wing supplementing the main rotor to achieve positive and negative load factors. Table 1 shows the distribution of the angle of attack, starting at its trim value of α_e before increasing to a value of $\alpha_0 + \alpha'$. This increase of angle of attack in the pull up stage of the manoeuvre increases the wing's lifting force helping the vehicle create a positive load factor. Similarly in the pushover stage of the manoeuvre the wing helps create a negative load factor. The value of α' is taken to be $8°$ in the current work which results in the wing providing a significant portion of the vehicle in the climbing stage of the manoeuvre whilst maintaining an adequate stall margin. The angle of attack variation is described by a fifth order polynomial, similar to that of Equation 13, therefore the angle of attack time derivative $\dot{\alpha}$ is easily obtained through differentiation.

2.3.2 Accel-Decel Manoeuvre

The acceleration and deceleration manoeuvre starts with the aircraft in the hover. It then accelerates to a flight velocity of 50 kt before aggressively decelerating back to a stabilised hover. The objective of this manoeuvre is to examine the pitch and heave axis handling qualities[26]. As the initial heading of the aircraft is to be maintained throughout the manoeuvre, the track angle, χ, and heading rate, $\dot{\psi}$ is set to zero. The five boundary conditions of this manoeuvre are given in Table 2 with the assumption that the maximum flight velocity of 50 kt is reached at the half-way point. A fourth-order polynomial describes the flight velocity

$$(15) \qquad V(t) = b_0 t^4 + b_1 t^3 + b_2 t^2 + b_3 t + b_4$$

where b_0, b_1, b_2, b_3 and b_4 are coefficients which are determined by applying the boundary conditions. For this particular manoeuvre, $\dot{x} = V(t)$ whereas $\dot{y} = \dot{z} = 0$. The rate of change of the flight velocity is readily available through the differentiation of Equation (15),

Table 2. Accel-Decel Boundary Conditions.

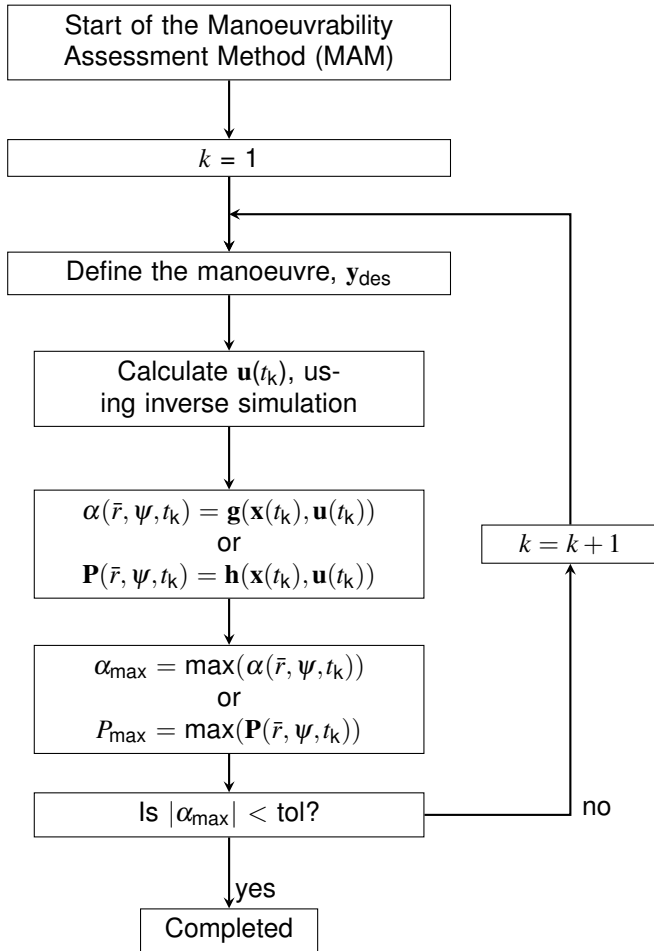| Variable	$t = 0s$	$t = t_{end}/2$	$t = t_{end}$
V	0	50 kt	0
$\dot{V}$	0	-	0

therefore allowing the calculation of the accelerations which are contained in the output vector, $\mathbf{y}_{des}$. The manoeuvre is defined by setting the distance to be travelled, S, obtained by integration of Equation (15) rather than specifying t_{end}.

Concerning the acceleration deceleration manoeuvre, the propeller pitch is scheduled throughout the manoeuvre so that the output vector consists of four elements, which are namely the three accelerations in the Earth axes set and the heading rate. As the propeller pitch is known throughout the manoeuvre, there are four unknown controls to calculate at each time point. The pitch schedule is developed to maximise the propeller thrust in the acceleration portion of the manoeuvre and is lowered in the deceleration segment. This manner of scheduling the propeller pitch is likely to be similar to the control strategy that the pilot would adopt to fully exploit the addition of propellers to the aircraft design. Of course, the pilot actively using five controls would undoubtedly increase the pilot workload throughout the manoeuvre. A solution to this issue could be a control system and interface, whereby the pilot has four available controls with a control system automatically altering the propeller pitch to increase propeller thrust in the acceleration segment of the manoeuvre. Such an investigation is not considered in the current work.

2.4 Manoeuvrability of the Configurations

The inverse simulation technique has been used to assess both the manoeuvrability and agility of helicopters[16,28]. In this current work, a similar approach to Whalley's is adopted[16], in order to assess the maximum manoeuvring capability of two helicopter configurations. However, there are some differences. Firstly, the integration method is used within this work unlike the differentiation technique used by Whalley[16]. The integration method allows for the inclusion of high fidelity modelling techniques, such as individual rotor blade modelling, which are not included within this study of compound helicopters but could be in future work.

Another important difference between Whalley's work and the current approach is the definition of the limiting factor which determines the aircraft's ability to complete a manoeuvre. There are various limits which define the manoeuvrability of a rotorcraft, which include

```
┌─────────────────────────────┐
│  Start of the Manoeuvrability │
│  Assessment Method (MAM)      │
└─────────────────────────────┘
            │
            ▼
┌─────────────────────────────┐
│           k = 1             │
└─────────────────────────────┘
            │
            ▼
┌─────────────────────────────┐
│  Define the manoeuvre, y_des │
└─────────────────────────────┘
            │
            ▼
┌─────────────────────────────┐
│  Calculate u(t_k), us-       │
│  ing inverse simulation      │
└─────────────────────────────┘
            │
            ▼
┌─────────────────────────────┐         ┌──────────────┐
│ α(r̄,ψ,t_k) = g(x(t_k),u(t_k)) │        │  k = k + 1   │
│           or                 │         └──────────────┘
│ P(r̄,ψ,t_k) = h(x(t_k),u(t_k)) │
└─────────────────────────────┘
            │
            ▼
┌─────────────────────────────┐
│ α_max = max(α(r̄,ψ,t_k))      │
│           or                 │
│ P_max = max(P(r̄,ψ,t_k))      │
└─────────────────────────────┘
            │
            ▼
┌─────────────────────────────┐   no
│    Is |α_max| < tol?         │──────────►
└─────────────────────────────┘
            │ yes
            ▼
┌─────────────────────────────┐
│        Completed            │
└─────────────────────────────┘
```

Fig. 3. Flowchart Describing the Manoeuvrability Assessment Method.

aerodynamic, power and control travel limits[29]. In Whalley's work[16] it is assumed that the maximum or minimum control angles are the limiting factor for the helicopter configuration to perform a particular manoeuvre. However, due to the assumption of linear aerodynamics within the current rotor model, and therefore not modelling blade stalling, the extreme limit of the main rotor collective can be reached, producing an unrealistic amount of rotor thrust. The first solution to this is to assume that the aerodynamic limitations of the main rotor determine the maximum manoeuvre capability of the vehicle. Hence, it is assumed that the limiting factor of certain manoeuvres occurs when the local angle of attack of the rotor blades, at a radial position $\bar{r} = 0.8$ is equal to 12° at any time point or azimuth position. The selection of the local maximum angle of attack of 12° is chosen as it is the limit before the onset of dynamic stall, whereas a radial position of $\bar{r} = 0.8$ represents the outer portion of the blades where the dynamic pressure

is high. These selected values of maximum local blade angle of attack and radial position have been altered in simulation runs to investigate their influence in the final manoeuvrability results. The analysis showed that as long as the radial position represented the outer portion of the rotor blades (i.e. $\bar{r} > 0.7$) then there was no significant difference in the final results. A similar result was found in the maximum local angle of attack selection, if the selected value was in the interval of 10-14°. An alternative approach is to assume that the power available restricts the vehicle's ability to complete a manoeuvre. This approach seems appropriate for certain manoeuvres which involve a compound helicopter. For example, in certain manoeuvres the wing offloads the main rotor and therefore it is unlikely that the aerodynamic restrictions of the main rotor would determine the vehicle's manoeuvrability. For these reasons, the manoeuvrability method allows the user to select their assumed limit which can based on main rotor aerodynamic restrictions or the power available.

Figure 3 presents an overview of the Manoeuvrability Assessment Method (MAM). This iterative method uses inverse simulation to determine the maximum manoeuvring capability of the two aircraft configurations. The method begins at the first iterative counter and subsequently defines the manoeuvre. Thereafter, the integration method calculates the control angles required to force the particular aircraft configuration along the desired flight path. With the controls and states calculated throughout the manoeuvre, the assumed limiting factor determining the vehicle's manoeuvrability can be calculated. If the limit is selected to be the aerodynamic restrictions of the main rotor then the local angle of attack at every time point, around the azimuth and at a radial position of $\bar{r} = 0.8$ is calculated. If $\alpha_{max} \leq 12$ at $\bar{r}$=0.8, throughout the manoeuvre, then the aggressiveness of manoeuvre is redefined until this condition is satisfied. Conversely, if the power available is the limiting factor then the total power throughout the manoeuvre is calculated and then the manoeuvre is redefined until MAM converges towards a solution. In terms of the Pullup-Pushover manoeuvre, the variable n_{max} is allowed to change to converge towards the manoeuvrability limit. Whereas with the Accel-Decel manoeuvre, the distance travelled by the vehicles, S, is allowed to vary to converge towards a solution.

3. RESULTS

3.1 Manoeuvrability Results

With the methodology developed, MAM can now be used to predict the manoeuvrability of two aircraft con-
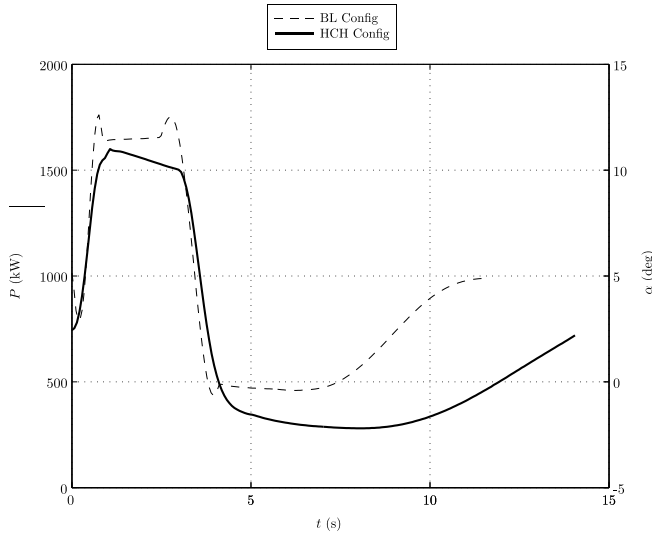
Fig. 4. Maximum Local Blade Angle of Attack Variation and Power during the Maximum Pullup-Pushover Manoeuvre.

figurations. For the Pull-Pushover manoeuvre, the assumed limiting factor which influences the HCH configuration's manoeuvrability is the power required. In the climbing portion of the manoeuvre, the wing offloads the main rotor, therefore it is unlikely that the main rotor's aerodynamic restrictions would be the limiting factor for this particular manoeuvre. Conversely, the aerodynamic restrictions of the main rotor is assumed to be

the BL configuration's limiting factor.

Concerning the BL configuration, Figure 4 presents the maximum calculated local blade angle of attack around the azimuth at each time point at the radial position, $\bar{r} = 0.8$. Also shown is the total power of the HCH configuration which is assumed to be limiting factor influencing the vehicle's manoeuvrability in this manoeuvre. As expected, the predicted limiting state of the BL configuration's main rotor occurs as the vehicle transitions to achieve its greatest normal load factor. In a similar manner the power of the HCH configuration reaches 1600kW at 1s which equals the power available, therefore predicting the vehicle's manoeuvrability. The load distributions achieved by each vehicle shown are Figure 5(a). The maximum load factors achieved by the HCH and BL configurations are 2.31 and 1.88, respectively. As a consequence the HCH configuration climbs to a greater height than the BL configuration, with the height profiles of the two configurations shown in Figure 5(b). The HCH configuration reaches a height of 140m after 7.7s whereas the BL configuration's maximum height is 87.7m is attained at 6.9s.

Figure 6 shows the control activity required throughout the maximum Pullup-Pushover manoeuvres. In the early stages of the manoeuvre, the main rotor collective of the two configurations take similar form, but less collective is required for the HCH configuration. The wing provides a significant portion of the overall vehicle

(a) Load Factor Distribution

(b) Height Profile
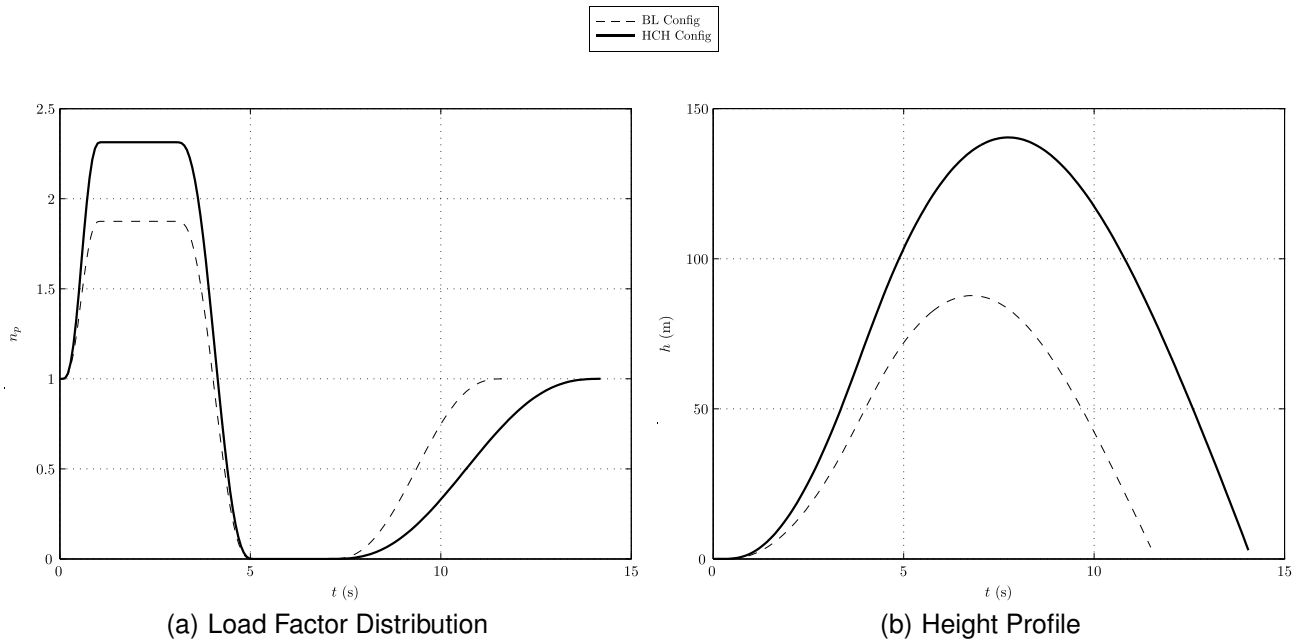
Fig. 5. Flight path during the Pullup-Pushover Manoeuvres.
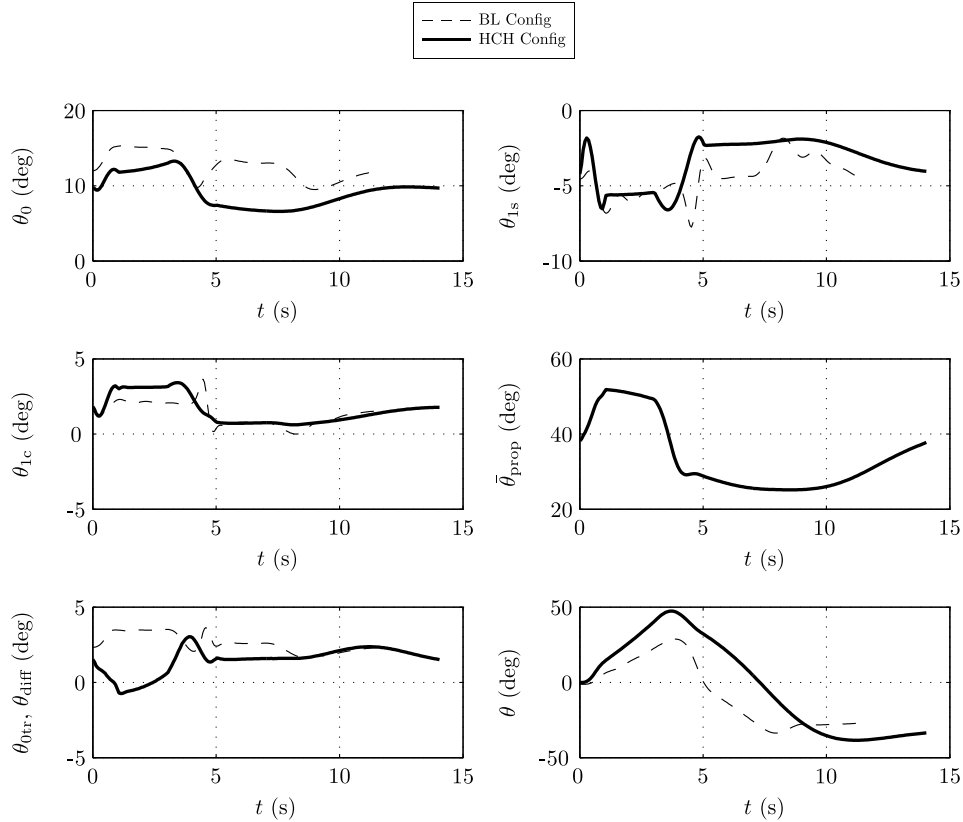
Fig. 6. Maximum Manoeuvrability Control time histories of the HCH and BL configurations during the Pullup-Pushover manoeuvre.

lift whereas the propellers provide the propulsive force. Therefore, the required rotor thrust of the HCH configuration is significantly less than that of the BL configuration, consequently lowering the main rotor collective. There are large negative longitudinal stick, θ_{1s}, inputs between 1-3s so that the two vehicles sustain their maximum load factors. As the vehicles transition to their minimum load factors, both assumed to be 0, the main rotor collective angles drop, however the BL configuration's main rotor collective drops less than that of the HCH configuration. The longitudinal cyclic of the BL configuration reaches its minimum value at 4.5s as it pitches down the aircraft to achieve a zero normal load factor. Note that the additional constraint featured in the HCH configuration, chosen to be the angle of attack, results in a more gradual change of pitch attitude when compared to the BL configuration. In terms of the propeller pitch, this control rises in the aggressive portion of the manoeuvre where the maximum load factor is attained. This of course increases the propeller thrusts to provide a significant propulsive force. As the aircraft transitions to a zero load factor, the propeller pitch reduces to a value of 31°, remaining within this region

until the latter stages of the manoeuvre. After 8s the propeller pitch begins to increases to recover the aircraft's forward flight speed.

For the Accel-Decel manoeuvre, the aerodynamic restrictions of the two main rotors are assumed to be limiting factor influencing the manoeuvrability of the two aircraft configurations. Figure 7 shows the maximum calculated blade local angle of attack around the azimuth at each time point at the radial position, $\bar{r}$ = 0.8. The two configurations reach their limiting states, i.e. α_{max}=12°, at approximately 1s, highlighting that MAM has successfully found a solution. This point corresponds to an aggressive part of the manoeuvre whereby there are large collective and longitudinal control inputs for both configurations to accelerate the vehicles from the hover. The predicted result is that the two aircraft configurations complete the manoeuvre in comparable time-scales, with the BL and HCH configurations completing the manoeuvre in 8.7s and 8.85s, respectively. Figure 8 shows the longitudinal distance travelled by the two vehicles, with the BL configuration completing the manoeuvre over a distance of 120.8m, whereas the HCH configuration covers a total distance

of 121.9m. This result suggests that there is little difference in the predicted maximum manoeuvrability capability whilst performing this manoeuvre. One possible reason for this is that the wing provides an aerodynamic download at these low flight speeds, requiring greater collective inputs in the early stage (between 0-1s) of the manoeuvre. Another explanation is the low levels of propeller thrusts required in the stabilised hover. As the manoeuvre commences the propeller collective, $\bar{\theta}_{prop}$, has to been increased significantly, which takes a few seconds, to provide a sizeable propulsive force. By the time the propellers produce significant axial thrust, ≈ 3s, there has already been large cyclic control pitch inputs which lead to the main rotor reaching its limiting state. However the addition of thrust compounding, featured in the HCH configuration, attenuates the pitch attitude excursions in the acceleration stage of the manoeuvre. This is clearly a beneficial aspect of the helicopter design.

Figure 9 presents the control time histories throughout the maximum Accel-Decel manoeuvres. As noted previously, the mean propeller pitch, $\bar{\theta}_{prop}$, is scheduled throughout this manoeuvre so that a unique solution can be determined at each time point but more importantly so that the HCH configuration exploits the benefit of thrust compounding. This manner of scheduling the propeller pitch allows the propulsive force of the two propellers to be controlled throughout the manoeuvre. The propeller pitch schedule, as seen in Figure 9, results in the two propellers providing a significant propulsive force in the early stages of the manoeuvre to provide axial acceleration, with the starboard and port pro-
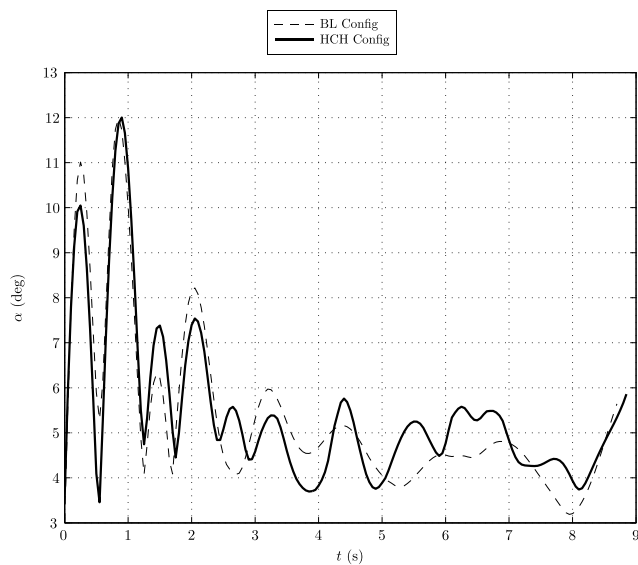

Fig. 7. **Maximum Local Blade Angle of Attack Variation during the Maximum Accel-Decel Manoeuvre.**
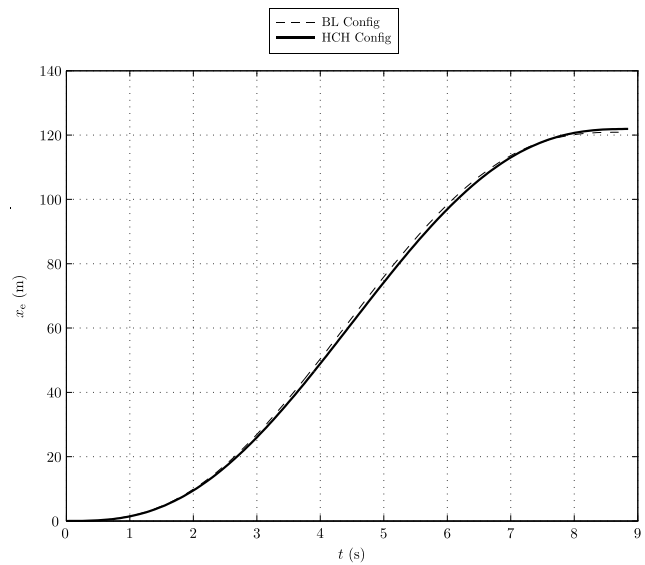
Fig. 8. **Flight path of the Maximum Accel-Decel Manoeuvres.**

pellers reaching maximum thrusts of 11.6kN and 6.4kN, respectively at the time of maximum acceleration. Note this manner of propeller pitch scheduling assumes that the no significant reverse thrust is used in the deceleration stage of the manoeuvre. At the starting position of the manoeuvre the main collective of the HCH configuration is greater than that of the BL configuration. This is due to wing of the HCH configuration providing an aerodynamic download which requires collective to offset the download force. As the manoeuvre commences, the main rotor collective of the two configurations increase with the collective of the BL configuration reaching its highest value at 4s. The HCH configuration's highest collective setting is reached at a much shorter time of 2s. When the main rotor collective of HCH configuration reaches its peak, the two propellers are producing a significant portion of the propulsive thrust to accelerate the aircraft. For a conventional helicopter the main rotor is responsible for both the propulsive and lifting capability of the vehicle[29]. One undesired quality of the helicopter is that in order to accelerate or decelerate a large pitch excursion is required. As a consequence, after 2s the main rotor disc of the HCH configuration does not have to tilt as much as the BL configuration in order to provide the propulsive force to the accelerate the vehicle. The net effect is that the pitch attitude is reduced, between 1-4s, when the pitch attitude of the two configurations are compared, highlighting one of the benefits of thrust compounding. The main rotor cyclic inputs are very similar throughout the manoeuvre. Both configurations exhibit large oscillatory longitudinal cyclic control inputs at the beginning of the
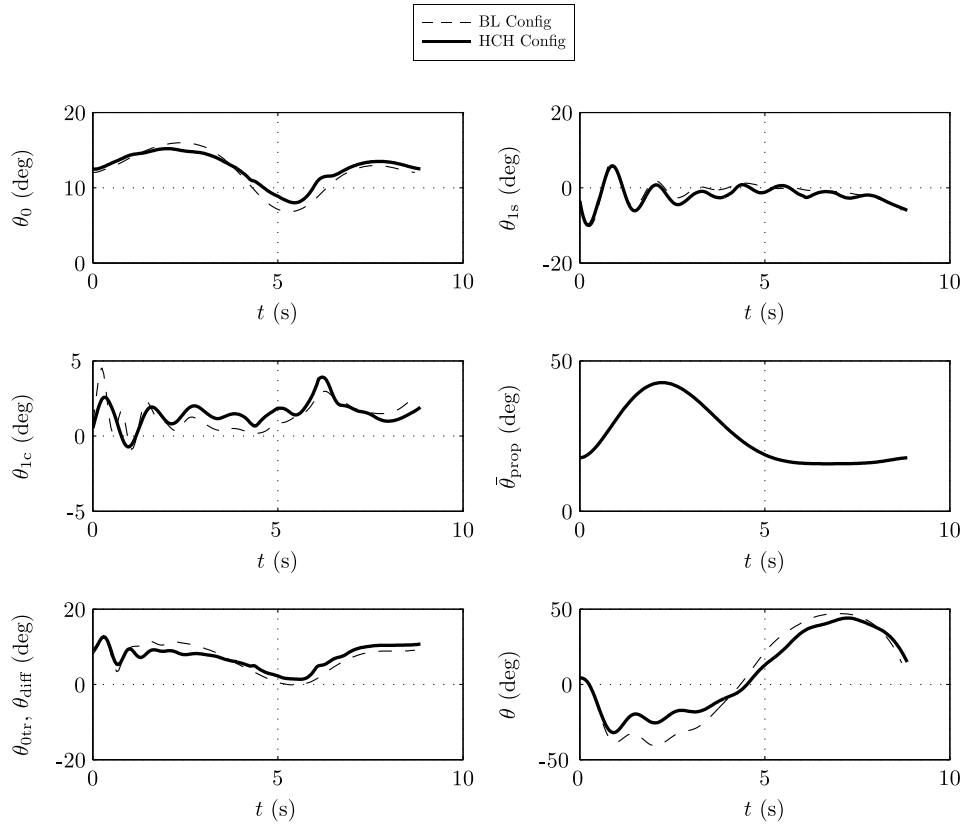
Fig. 9. Maximum Manoeuvrability Control time histories of the HCH and BL configurations during the Accel-Decel manoeuvre.

manoeuvre.In terms of the anti-torque controls, θ_{0tr} and θ_{diff}, their control time histories are similar to the collective settings in order for the aircraft to retain a constant heading.

CONCLUSIONS

The manoeuvrability of a hybrid compound helicopter and a conventional helicopter have been examined. The following is a list of the main conclusions drawn from this work:

- A preliminary manoeuvrability assessment of a hybrid compound helicopter has been conducted. When comparing the main rotor collective displacements of the configurations throughout the Pullup-Pushover manoeuvre, the HCH configuration requires less main rotor collective than the BL configuration. This is due to the wing offloading the main rotor as the aircraft climbs to achieve a positive load factor and the two propellers providing significant propulsive thrust. The combination of these two types of compounding reduces the amount of

rotor thrust required therefore lowering the amount of main rotor collective required. Concerning the HCH configuration, the introduction of the additional constraint, $\dot{\alpha}$, results in a gradual change in pitch attitude as the aircraft transitions from the maximum load factor to the minimum. In terms of manoeuvrability, the HCH configuration is able to achieve a greater load factor than the BL configuration. This is primarily due to the combination of thrust and wing compounding offloading the main rotor's propulsive and lifting duties throughout the manoeuvre.

- For the Accel-Decel manoeuvre, the cyclic control activity of the two configurations is similar throughout the manoeuvre. The addition of thrust compounding lowers the required pitch attitude of the vehicle in the forward acceleration stage of the manoeuvre as expected. As the main rotor does not have to provide the propulsive force the tilt of the rotor disc is smaller than that of the BL configuration, attenuating the pitch attitude. Regarding the manoeuvrability of the two configurations, there is little

difference in the predicted maximum manoeuvrability of the two vehicles performing this manoeuvre. This is due to the large longitudinal stick inputs of the two configurations in the early stages of the manoeuvre. These control inputs lead to the estimated limiting state of the two main rotors.

ACKNOWLEDGEMENTS

COPYRIGHT STATEMENT

REFERENCES

[1] M.N. Orchard and S.J. Newman. The compound helicopter - why have we not succeeded before? *The Aeronautical Journal*, 103(1028):489–495, 1999.

[2] Douglas Thomson and Roy Bradley. Inverse simulation as a tool for flight dynamics research - Principles and applications. *Progress in Aerospace Sciences*, 42(3):174–210, May 2006. ISSN 03760421. doi: 10.1016/j.paerosci.2006.07.002. URL http://linkinghub.elsevier.com/retrieve/pii/S0376042106000479.

[3] D.G. Thomson and R. Bradley. An analytical method of quantifying helicopter agility. In *Proceedings of the 12th European Rotorcraft Forum*, Garmisch-Partenkirchen, 1986.

[4] D.G. Thomson and R.B. Bradley. An investigation of pilot strategy in helicopter nap-of-the-earth manoeuvres by comparison of flight data and inverse simulation. In *Royal Aeronautcal Society: helicopter handling qualities and control*, London, 1988.

[5] D.G. Thomson and R. Bradley. The use of inverse simulation for conceptual design. In *16th European Rotorcraft Forum*, Glasgow, 1990.

[6] D.G. Thomson and R. Bradley. The use of inverse simulation for preliminary assessment of helicopter handling qualities. *The Aeronautical Journal*, 101 (1007):287 – 294, 1997.

[7] N. Cameron, D.G. Thomson, and D.J. Murray-Smith. Pilot modelling and inverse simulation for initial handling qualities assessment. *The Aeronautical Journal*, 107(1074):511– 520, 2003. ISSN 0001-9240.

[8] R.A. Hess, C. Gao, and S.H. Wang. Generalized technique for inverse simulation applied to aircraft maneuvers. *Journal of Guidance, Control and Dynamics*, 14(5):920–926, 1991. doi: 10.2514/3.20732.

[9] R.A. Hess and C. Gao. A Generalized Algorithm for Inverse Simulation Applied to Helicopter Maneuvering Flight. *Journal of the American Helicopter Society*, 38(4):3 – 15, 1993. doi: 10.4050/JAHS.38.3.

[10] G. Avanzini and G. de Matteis. Two-timescale inverse simulation of a helicopter model. *Journal of Guidance, Control and Dynamics*, 24(2):330–339, 2001. doi: 10.2514/2.4716.

[11] R. Celi. Optimization-Based Inverse Simulation of a Helicopter Slalom Maneuver. *Journal of Guidance, Control and Dynamics*, 23(2):289–297, 2000. doi: 10.2514/2.4521.

[12] G. de Matteis, L.M. de Socio, and A. Leonessa. Solution of Aircraft Inverse Problems by Local Optimization. *Journal of Guidance, Control and Dynamics*, 18(3):567–571, 1995. doi: 10.2514/3.21424.

[13] J.R. Olson and M.W. Scott. Helicopter Design Optimization for Maneuverability and Agility. In *American Helicopter Society 45th Annual Forum*, Boston, MA, 1989.

[14] K.L. Johnson. *Prediction of Operational Envelope Maneuverability Effects of Rotorcraft Design*. Ph.d, Georgia Institute of Technology, 2013. URL http://hdl.handle.net/1853/47601.

[15] L.S. Levine, F.W. Warburton, and H.C. Curtiss Jr. Assessment of Rotorcraft Agility and Maneuverability with Pilot-in-the-loop Similation. In *American Helicopter Society 41st Annual Forum*, Fort Worth, TX, 1985.

[16] M.S. Whalley. Development and Evaluation of an Inverse Solution Technique for Studying Helicopter Maneuverability and Agility. USAAVSCOM TR 90-A-008, 1991.

[17] G.D. Padfield. *Helicopter Flight Dynamics: the Theory and Application of Flying Qualities and Simulation Modelling*. Blackwell Publishing, 2nd edition, 2007. ISBN 13:978-1-4051-1817-0.

[18] K.M. Ferguson and D.G. Thomson. Flight dynamics investigation of compound helicopter configurations. *Journal of Aircraft*, AIAA Early Edition, 2014. doi: 10.2514/1.C032657.

[19] D.G. Thomson. Development of a Generic Helicopter Mathematical Model for Application to Inverse Simulation. Internal Report No. 9216, Department of Aerospace Engineering, University of Glasgow, UK, 1992.

[20] S. Rutherford. *Simulation Techniques for the Study of the Manoeuvring of Advanced Rotorcraft Configurations*. Phd thesis, University of Glasgow, 1997.

[21] M.H. Mansur. Development and Validation of a Blade Element Mathematical Model for the AH-64A Apache Helicopter. NASA-TM-108863, 1995.

[22] S.S. Houston. Validation of a non-linear individual blade rotorcraft flight dynamics model using a perturbation method. *The Aeronautical Journal*, 98 (977):260–266, 1994.

[23] R. Bradley, G.D. Padfield, D.J. Murray-Smith, and D.G. Thomson. Validation of helicopter mathematical models. *Transactions of the Institute of Measurement and Control*, 12(186), 1990. doi: 10.1177/014233129001200405.

[24] S. Rutherford. *Simulation Techniques for the Study of Advanced Rotorcraft*. Phd, University of Glasgow, 1997.

[25] D.G Thomson and R.B. Bradley. Mathematical Definition of Helicopter Maneuvers. *Journal of the American Helicopter Society*, 4(1):307 − 309, 1997. doi: 10.4050/JAHS.42.307.

[26] Anon. Handling qualities requirements for military rotorcraft. Aeronautical design standard ADS-33E-PRF, United States army aviation and troop command, 2000.

[27] R. Celi. Analytical Simulation of ADS-33 Mission Task Elements. In *American Helicopter Society 63rd Annual Forum*, Virginia Beach, VA, 2007.

[28] Douglas Thomson. *Evaluation of helicopter agility through inverse solution of the equations of motion*. Ph.d, University of Glasgow, 1987.

[29] J.G. Leishman. *Principals of Helicopter Aerodynamics*. Cambridge University Press, 2nd edition, 2006. ISBN 978-0-521-85860-1.